Spatial evolution of cooperation with variable payoffs

Cite as: Chaos **32**, 073118 (2022); https://doi.org/10.1063/5.0099444
Submitted: 17 May 2022 • Accepted: 16 June 2022 • Published Online: 12 July 2022

Ziyan Zeng, Qin Li and Minyu Feng

Spatial evolution of cooperation with variable payoffs

Cite as: Chaos **32**, 073118 (2022); doi: 10.1063/5.0099444
Submitted: 17 May 2022 · Accepted: 16 June 2022 ·
Published Online: 12 July 2022

Ziyan Zeng,[1] Qin Li,[2] and Minyu Feng[1,a)]

AFFILIATIONS

[1]The College of Artificial Intelligence, Southwest University, No.2 Tiansheng Road, Beibei, Chongqing 400715, China
[2]School of Public Policy and Administration, Chongqing University, No.174 Shazhengjie, Shapingba, Chongqing 400044, China

[a)]**Author to whom correspondence should be addressed:** myfeng@swu.edu.cn

ABSTRACT

In the evolution of cooperation, the individuals' payoffs are commonly random in real situations, e.g., the social networks and the economic regions, leading to unpredictable factors. Therefore, there are chances for each individual to obtain the exceeding payoff and risks to get the low payoff. In this paper, we consider that each individual's payoff follows a specific probability distribution with a fixed expectation, where the normal distribution and the exponential distribution are employed in our model. In the simulations, we perform the models on the weak prisoner's dilemmas (WPDs) and the snowdrift games (SDGs), and four types of networks, including the hexagon lattice, the square lattice, the small-world network, and the triangular lattice are considered. For the individuals' normally distributed payoff, we find that the higher standard deviation usually inhibits the cooperation for the WPDs but promotes the cooperation for the SDGs. Besides, with a higher standard deviation, the cooperation clusters are usually split for the WPDs but constructed for the SDGs. For the individuals' exponentially distributed payoff, we find that the small-world network provides the best condition for the emergence of cooperators in WPDs and SDGs. However, when playing SDGs, the small-world network allows the smallest space for the pure cooperative state while the hexagon lattice allows the largest.

The evolution dynamics in human population reveals how the cooperative behaviors emerge in society. Abundant previous studies have proposed different social dynamic mechanisms and explained the formation of cooperators in the networked population. In a population with networked relationship, the vertices present players that participant in the evolutionary game, and the edges denote the reciprocal relation. Recently, the concept of variable payoff in the evolutionary game theory has provided a new perspective for a better understanding of the cooperation.[1,2] To further investigate the evolutionary cooperation in the structured population, we introduce the stochastic variables to the spatial structures and study the cooperation frequency and formation in lattices and small-world networks.

I. INTRODUCTION

Understanding the evolution of cooperation has been a long-debate task since Darwin,[3,4] where the past studies built the research framework as the evolutionary game theory.[5,6] When the individuals make decisions, the social dilemmas occur in populations because of the conflict of partial and global interests.[7] One common evolutionary game model is the prisoner's dilemma,[8] in which people can choose to be cooperators or defectors. The cooperators bring the whole population high earnings while the defectors only lead to their own success. There has been research showing that the only Nash equilibrium of the prisoner's dilemmas is the defection in the well mixed populations,[9] but fortunately, Nowak and May first brought spatial chaos into the weak prisoners dilemmas (WPDs) and found that the cooperators emerge as long as the individuals are in spatial structures.[10] Thereafter, numerous studies presented the emergence of cooperators in network structures for various social dilemmas.[11] However, the study by Hauert and Doebeli on the SDGs showed that the spatial structure does not always promote the cooperative behaviors,[12] but often inhibits the evolution of cooperation. Later, Santos and Pacheco found that the scale-free networks substantially promote the outbreak of cooperators for both the WPDs and the SDGs whatever the network parameter is.[13] Besides, since the proposal of the five rules for the evolution of cooperation,[14] the research on human cooperation has sprung up to understand the formation of human behaviors.[15]

In the past decade, many complex network models emerge as the times require,[16] including the multi-layer networks,[17,18] the temporal networks,[19,20] and the higher-order networks.[21,22] These innovative network models provide the population structure for the research of the spatial evolutionary games.[23] On the multi-layer networks, the studies focus on how the couple of each network influence the cooperative behaviors,[24] and the population structures are regarded as the networks of networks.[25] On the temporal networks, the current studies focus on the change of the network edges and the cooperation density,[26] where the interaction relationships can be time-varying.[27] On the higher-order networks, the existing studies pay attention to the influence of the higher-order structure on the cooperative behaviors,[28,29] and the interaction process is extended from the individual-to-individual pattern to the group-to-group pattern. The existing studies on these novel network types have been already concluding that the cooperative behaviors emerge in different forms and network structures.[23] For example, Zhang *et al.* studied the spatial public goods game on two-layered lattices,[30] finding that much stronger learning preference will override the role of interdependency in the evolution of cooperation. Han *et al.* studied the evolutionary public goods game model in an activity-driven network.[31] Civilini *et al.* studied the evolutionary game model of group choice dilemmas on hypergraphs,[32] which can explain the emergence of irrational herding and radical behaviors in social groups.

Over the past years, studies are concentrating on the evolution of cooperation with some stochastic phenomenons in real society. For example, Su *et al.* recently studied the evolution of cooperation with game transitions,[33] finding that the game transitions can significantly reduce the critical benefit-to-cost threshold for cooperation. Perc studied the coherence resonance in the spatial prisoner's dilemmas,[34,35] which introduced the white noises to the individuals' payoff for square lattices in the social dilemmas. Zeng *et al.* introduced the individual's stochastic birth and death to the spatial evolutionary game model,[36,37] finding that the spatial inheritance[38] enhances the cooperation if each individual's lifespan are limited in the Poisson growing complex networks.[39,40]

In real systems, agents' payoffs are usually not immutable and frozen as they interact with others in the evolutionary games. Commonly, the payoffs are floating around some empirical values. Therefore, in this paper, we mainly focus on the variable payoffs and stochastic risks in the evolution of cooperation. Consequently, we presume that individuals' payoffs follow a specific probability distribution. Each player can get higher or lower payoffs than the expectation, leading to both unpredictable chances and risks in the spatial evolution of cooperation. In our model, the standard deviation of the probability distribution can be regarded as the risk one may possess. Our work introduces the stochastic risks in the evolution of cooperation and helps to understand the effect of variable payoffs in human society. In simulations, we mainly pay attention to the cooperation density, the strategy formation, and the individuals' payoffs at the network's stable state. Additionally, we emphasize that the concept of variable payoffs in the evolution of cooperation is not new.[1] For example, Perc and Szolnoki studied the diversity in wealth and social status and found that the distribution of wealth and social status might have played a crucial role.[41] Amaral *et al.* studied the spatial evolutionary game where the game played at each interaction is drawn uniformly at random, highlighting the favorable role of heterogeneity regardless of its origin.[42] Nevertheless, our results show new conclusions for the promotion of cooperation with the individuals' variable payoffs.

This paper is organized as follows. In Sec. II, we introduce our game model with the stochastic risks. In Sec. III, we show our simulation results on cooperation density. In Sec. IV, we conclude our work.

II. MODEL

In real systems, the payoffs that agents obtain from each other in the evolution of cooperation are usually fluctuating instead of constant. In this section, we introduce the spatial evolutionary game model under variable payoffs. Generally, in the game model with two players and two strategies, both individuals receive R on the mutual cooperation and P on the mutual defection. Additionally, the one-way cooperation yields T for the defector and S for the cooperator. Specifically, we consider the weak prisoner's dilemma (WPD) with $R = 1$, $T = b$, $P = S = 0$ and the snowdrift game (SDG) with $R = 1$, $S = 1 - r$, $T = 1 + r$, $P = 0$. In the networks, each vertex presents an individual, and each edge presents the relationship between two individuals, and each individual only interacts with their neighbors. We suppose that an individual's payoff can be a random variable that follows a certain probability distribution but has a fixed expectation, which leads to a random fluctuation risk when the individuals interact with their neighbors. Additionally, the standard deviation of the payoff is regarded as the risk of the interaction, inducing that each individual has both the chance to obtain a higher payoff than the expectation and the risk to get a lower payoff. Concretely, we consider two kinds of probability distributions, including the normal and the exponential distribution. The normal distributed payoff allows individuals to obtain higher or lower payoffs than the expectation with the same probability. Additionally, in this case, the variance is independent of the payoff. The exponential distributed payoff provides a high probability for the individuals to get higher or lower payoffs if the expectation is high. In the following contents, we primarily introduce the normal distributed payoff model. Then, we introduce the exponential distributed payoff model. Subsequently, we illustrate the strategy update rule.

A. Normal distributed payoffs

As is well known, the normal distributions have been found in many real situations for the individuals' payoffs.[43] The first probability distribution that we introduce for the individual's payoff is the normal distribution. The normal distributed payoff has a fixed standard deviation value (σ) and is independent of the expectation. Therefore, the random payoff that an individual gets is not related to the expected payoff. We assume that an individual's payoff from a neighbor, say x, follows the normal distribution denoted as

$$f(x, \mu, \sigma) = \frac{1}{\sqrt{2\pi}\sigma} \exp\left(-\frac{(x-\mu)^2}{2\sigma^2}\right), \tag{1}$$

herein μ is the expectation and σ indicates the standard deviation. According to our assumption, the payoff matrix of the WPD with

the normal distributed payoff can be defined as

$$M_1 = \begin{pmatrix} N(1,\sigma) & N(0,\sigma) \\ N(b,\sigma) & N(0,\sigma) \end{pmatrix}, \tag{2}$$

where $1 < b \leq 2$ is a flexible parameter, and the SDG is defined as

$$M_2 = \begin{pmatrix} N(1,\sigma) & N(1-r,\sigma) \\ N(1+r,\sigma) & N(0,\sigma) \end{pmatrix}, \tag{3}$$

herein $0 \leq r \leq 1$. $N(\mu,\sigma)$ in Eqs. (2) and (3) denotes the random number operator for the normal distribution with the parameters μ and σ in Eq. (1). μ is the game parameter in classical game models, and σ describes the deviation degree from the expected payoff. Besides, x denotes the payoff that an individual obtains.

It is worth noting that the WPDs are not typical prisoner's dilemmas and there are some differences. According to the definition of the normal distribution, a smaller σ ensures a lower probability to obtain a greater or smaller payoff and makes the player's income relatively stable. However, if the deviation σ is large, the players may have more opportunities to obtain both the improved payoff and the reduced payoff, which brings agents both the chances and the risks.

B. Exponential distributed payoffs

Next, we assume that if one tries to earn more, the risk will be higher as well, which is a common rule in real societies. We propose to use the exponential distributed variables to describe the payoffs in the evolution of cooperation. The risk of the exponential distributed payoff is related to the expectation and is higher if the payoff is higher as well. The exponential probability density function has two writing styles. In this paper, we presume an individual's payoff x from one neighbor follows the probability distribution denoted as

$$f(x,\theta) = \frac{1}{\theta}\exp -\frac{x}{\theta}, \quad x > 0, \tag{4}$$

where θ is the expectation. Additionally, θ^2 is the variance of each individual's payoff. Accordingly, as the increase of θ, the fluctuation is more unstable. The payoff matrix of the WPD with the exponential distributed payoff can be defined as

$$M_3 = \begin{pmatrix} E(1) & E(\xi) \\ E(b) & E(\xi) \end{pmatrix}, \tag{5}$$

and the SDG as

$$M_4 = \begin{pmatrix} E(1) & E(1-r) \\ E(1+r) & E(\xi) \end{pmatrix}, \tag{6}$$

herein $E(\theta)$ denotes a random number that follows the exponential distribution with the parameter θ in Eq. (4), and b, r are defined the same as above. ξ is a tiny number to ensure the exponential distribution is meaningful.

We emphasize again that the standard deviation changes as the expected payoff, i.e., the payoff fluctuation level floats as the game parameters. the fluctuation. Besides, the standard deviation is higher than 1 if the individual's payoff is greater than 1. Therefore, when the individuals try to obtain a higher payoff than the mutual cooperation, both the chance and risk increase as the payoff does.

C. Strategy update

Agents in the evolutionary game often pursue higher returns. Therefore, we consider that each individual learns the profitable strategies among its neighbors. In one time step, all individuals calculate their total payoffs, say Π_x for the individual x, by summing their returns from the neighbors. Then, each individual in the network randomly selects a neighbor and compare their payoffs. If a player x with the payoff Π_x randomly selects her neighbor y with the payoff Π_y, the player x tries to imitate the player y's strategy if and only if $\Pi_y > \Pi_x$ with the probability

$$W(x \leftarrow y) = \left[\frac{\Pi_y - \Pi_x}{D\max(k_x,k_y)}\right]_0^1, \tag{7}$$

where $D = b$ in the WPDs, and $D = 1 + r$ in the SDGs. If $\Pi_y \leq \Pi_x$, the player x does not study its neighbor y's strategy. The denominator $D\max(k_x,k_y)$ is the normalized item in numerous previous studies. However, we further define the operator $[\cdot]_0^1$ as

$$[a]_0^1 = \begin{cases} 0, & a < 0, \\ a, & 0 \leq a \leq 1, \\ 1, & a > 1. \end{cases} \tag{8}$$

The reason why we adopt this operator is that the probability may be greater than 1 and less than 0 because of the variable payoff, and once this happens, we need to transfer the result to ensure the nature of the probability.

III. RESULT

In this section, we present our simulation results on cooperation density to show how cooperative behaviors vary with different game parameters. We mainly focus on the cooperation density, the cooperative cluster formations, and the population payoff distribution at the evolution stable state. We perform the simulation on four network types, including the hexagonal lattices (HL, 36×36, $N = 2592$), square lattices (SL, 50×50, $N = 2500$), Watts–Strogatz small-world networks (SW, $N = 2500$, $k = 8$, $p = 0.4$), and triangular lattices (TL, 70×70, $N = 2450$) with the periodic boundary, to ensure that the network sizes are approximately 2500, which guarantees that the cooperator density is barely affected by the network sizes. Each individual is set to be a cooperator or a defector with the same probability of 50%. According to our simulation, the evolution process is stable after the 4500th time step. Therefore, we calculate the cooperation density by averaging each cooperation density from the 4500th step to the 5000th step in all following simulations. All simulation results are carried out on *Python*. All networks are generated by the function *networkx.generators.lattices* in the project *Networkx*. Besides, the normal distributed and exponential distributed variables are generated by the function *numpy.random.normal* and *numpy.random.exponential*, respectively, in the project *Numpy*. And, the cooperation density (f_c) is the percentage of cooperators in the whole population.

A. Payoffs following the normal distribution

As stated previously, we consider the evolution of population strategy with individuals' payoffs that follow different probability

distributions. We first display the results with individuals' normal distributed payoffs for the WPDs and SDGs.

1. Cooperation density

(a) WPDs. Primarily, we present the cooperation density results for the WPDs in the parameter space (b, σ) with individuals' normal distributed payoffs. The defector's temptation b and the standard deviation σ are in the range $(1, 2]$ and $[0, 1)$, respectively. In Fig. 1, we show the cooperation density heatmaps in the game parameter space (b, σ). Since the cooperation density varies on the different network structures, we set the different y axis ranges for each network type for a better presentation.

As is shown in Figs. 1(a) and 1(b), there is no pure cooperative strategy formation even if the defector's temptation is small. Only mixed and pure defective states exist in the parameter space. The HL and the SL are fully occupied by the defectors if the defector's temptation $b > 1.10$ and $b > 1.15$, respectively. Therefore, we can say that the SL allows more cooperators than the HL. Besides, the HL and the SL provide the highest cooperation annihilation threshold (the maximum game parameter for the emergence of cooperators) as σ is around 0.22 and 0.12 separately, where the greater or lower σs allow the smaller spaces for the cooperation.

In Figs. 1(c) and 1(d), it is obvious that the SW and the TL provide more cooperators to the population than the HL and the SL, and there are pure cooperative states. Besides, the SW promotes the cooperative behaviors for the most parameter space and provides the best condition for pure cooperation, where the defection presence threshold (the minimum game parameter for the defectors to emerge) is the highest. Additionally, for the SW, the cooperators may emerge provided $b < 1.60$, while for the HL, no cooperator exists in the population provided $b > 1.28$. And, the cooperation annihilation threshold decreases with the increase of the standard deviation σ. Although in the HL and the SL, the cooperation behaviors are enhanced if σ is small, we can say that a higher σ usually inhibits the emergence of cooperation in the spatial WPDs with the four network types we consider. Besides, the SW provides the best condition for cooperative behaviors, while the HL provides the worst.

(b) SDGs. With the same network sizes as above, we next present the cooperation density for the SDGs in the game parameter space (r, σ). As is shown in Figs. 2(a), 2(b), and 2(d), the HL, the SL, and the TL allow more spaces for the pure cooperative states with a greater σ, i.e., the greater standard deviation σ leads to a steeper phase transition between the pure cooperation and the pure defection as the increase of r. Additionally, the HL provides both the most and least parameter space for the pure cooperation and the mixed state, respectively. However, in the SW, the cooperation density is hardly affected by the standard deviation σ. Besides, the SW allows more symbiotic space for cooperation and defection, which inhibits the emergence of pure defection in the population. In the HL, the cooperation annihilation threshold is decreased with the increase of r, bringing less space for the mixed state with both the cooperators and the defectors.

Nevertheless, the cooperation annihilation thresholds of the SL, the SW, and the TL are relatively stable, ensuring that the condition for the pure defection barely changes if the standard deviation σ is different. Therefore, we can say that a high standard deviation σ usually promotes the emergence of spatial cooperative behaviors in the four network types we consider.

2. Cooperation snapshots in SLs

To investigate the formation of cooperative behaviors with the individuals' payoffs that follow the normal distribution, we present the snapshots for both the WPD and the SDG in the SLs with the size $N = 50 \times 50$ in Figs. 3 and 4. Each individual is set as a cooperator or defector with the probability of 50%. To ensure the stationary state of the networks, we observe the cooperation snapshots at $t = 5000$. The blue and white cells present the cooperators and the defectors separately.

(a) WPDs in SLs. To start with, we show the cooperation snapshots in Fig. 3 for the WPDs by setting $b = 1.02, 1.03, 1.04$ and $\sigma = 0.10, 0.30, 0.50, 0.70$ for the cross simulations. For all the defector's temptation we presume, as σ changes from 0.10 to 0.30,

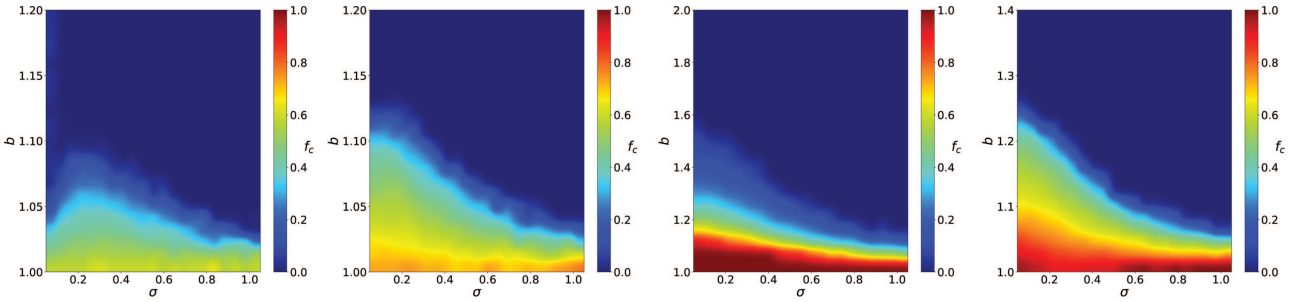

FIG. 1. Cooperation heatmaps of WPDs. Cooperative behaviors are usually enhanced with a low standard deviation in WPDs. This figure presents the cooperation density for the WPDs with individuals' normal distributed payoff on HL [1(a)], SL [1(b)], SW [1(c)], and TL [1(d)]. We set the x axis as the standard deviation σ with the range [0, 1.0] and the y axis as the defector's temptation b with the range (1.0, 1.2] in 1(a) and 1(b), (1.0, 2.0] in 1(c) and (1.0, 1.4] in 1(d). Each cooperation density is obtained by averaging the last 500 evolution steps in the 5000 total steps. The cooperation density (f_c) is high with a warm color in the parameter spaces.

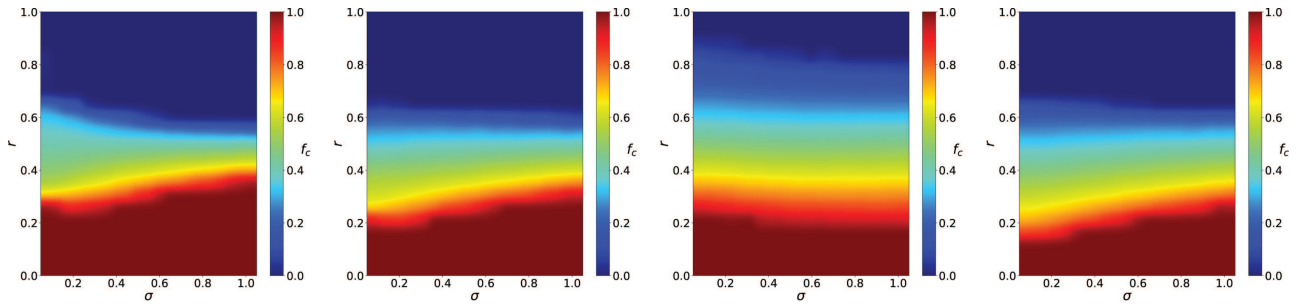

FIG. 2. Cooperation heatmaps of SDGs. Cooperative behaviors are usually enhanced with a high standard deviation in SDGs. This figure presents the cooperation density for the SDGs with individuals' normal distributed payoff on HL [2(a)], SL [2(b)], SW [2(c)], and TL [2(d)]. We set the x axis as the standard deviation σ with the range [0, 1.0] and the y axis as the cost-to-benefit ratio ratio r in each figure. Each cooperation density is obtained by averaging the last 500 evolution steps in the 5000 total steps. The cooperation density (f_c) is high with a warm color.

the cooperation densities decrease slightly, and only a small number of cooperation clusters split. For the temptation $b = 1.02$ [Figs. 3(a)–3(d)], as σ increases from 0.30 to 0.70 and 0.90, the cooperation density reduces moderately. However, for the temptation $b = 1.03$ [Figs. 3(e)–3(h)] and 1.04 [Figs. 3(i)–3(l)], the cooperators reduce substantially if the standard deviation σ increases. Specifically, provided $b = 1.02$ and $\sigma = 0.10$, the cooperation density we obtain at $t = 5000$ is 0.6500. With the increase of σ, the cooperation density reduces to 0.6388 for $\sigma = 0.30$, 0.4776 for $\sigma = 0.70$, and 0.3372 for $\sigma = 0.90$. When we set $b = 1.03$ and 1.04, the cooperation density becomes more sensitive to the standard deviation σ. For the defector's temptation $b = 1.03$, if $\sigma = 0.10$, the cooperation density of the corresponding snapshot is 0.6248. As σ changes from 0.10 to 0.30, the cooperation density becomes 0.5828, and as σ increases to 0.70 and 0.90, the corresponding cooperation proportions reduce to 0.4012 and 0.2316, respectively. For the defector's temptation $b = 1.04$, if $\sigma = 0.10$, the cooperation density is 0.6172. As σ increases to 0.30, 0.70, and 0.90, the cooperation densities drop to 0.5736, 0.3144, and 0.0796 separately with a sharp decline. Generally, the clusters of the cooperators are disintegrated with the increase of the standard deviation σ when the individuals play the WPDs.

There have been numerous previous studies indicating that the network structure helps to build up the cooperative clusters and then defend the invasion of the defectors because each agent has to play the same cooperative strategy with its neighbors to maintain the considerable mutual income. However, as shown by the snapshots on SLs, with the same defector's temptation b, the population is more likely to split the cooperation clusters with a large standard deviation σ. Considering an already formed cooperative cluster, if the payoff they get is higher than the expectation (or just relatively high), the cooperative cluster is stable. However, once an individual gets only a small payoff and even smaller than the defector's among its neighbor, there will be an instantaneous disintegration for the cooperative cluster, which is hard to reconstitute. Besides, the higher σ makes the cooperative clusters easier to split but harder to reconstruct. Therefore, a high standard deviation σ usually brings more defectors to the population. Additionally, there is an equilibrium between the decomposition and reconstruction of cooperative clusters, ensuring that the population strategy combination can be relatively stable in our simulations. And, as shown by the snapshots on SLs, with the same defector's temptation b, the population is more likely to split the cooperation clusters with a large standard deviation σ.

(b) SDGs in SLs. Next, we show the snapshots for SDGs on SLs in Fig. 4. We set the game parameter $r = 0.25, 0.35, 0.55$ and $\sigma = 0.10, 0.30, 0.70, 0.90$ for the cross simulations. Generally, for $r = 0.25$ [Figs. 4(a)–4(d)] and 0.35 [Figs. 4(e)–4(h)], the cooperation densities rise prominently as the increase of the standard deviation σ, and for $r = 0.55$ [Figs. 4(i)–4(l)] there is also a slight increase as σ increases in contrary to the WPDs. For the cost-to-benefit ratio $r = 0.25$, the cooperation density for $\sigma = 0.10$ is 0.6948. As the standard deviation σ increases to 0.30, the cooperation proportion is increased as well to 0.7644. For $\sigma = 0.70$ and 0.90, the individuals reach a pure cooperative state, where the cooperation density is 1 and can be regarded as a steep increase. For the cost-to-benefit ratio $r = 0.35$, the cooperation density we obtain for $\sigma = 0.10$ is 0.5532, and it rises to 0.5880 if $\sigma = 0.30$. When the standard deviation $\sigma = 0.70$ and 0.90, the corresponding cooperation densities are 0.6476 and 0.7136, respectively. Obviously, the upward trend for $r = 0.35$ is smaller than $r = 0.25$ as the standard deviation σ increases. For $r = 0.55$, the cooperation densities are 0.2848 and 0.3008 separately for the standard deviation $\sigma = 0.10$ and 0.30. With the increase of σ, the cooperation densities are almost unchanged, and the cooperation proportions we obtain are 0.3132 and 0.3084 for $\sigma = 0.70$ and 0.90, respectively. Generally, in opposition to the results in WPDs, the cooperative clusters grow with the increase of the standard deviation σ if the individuals play the SDGs.

In previous studies, it has been shown that the individuals in SDGs often form the filamentous cooperation clusters because the individuals tend to play the opponent's counter-strategy. If the cost-to-benefit ratio is higher, the defectors are more likely to invade the population and bring down the cooperation density. According to our simulation results, a high standard deviation σ usually brings more cooperators to the population if the cost-to-benefit ratio r is small. Besides, a higher σ promotes the cooperators to form more

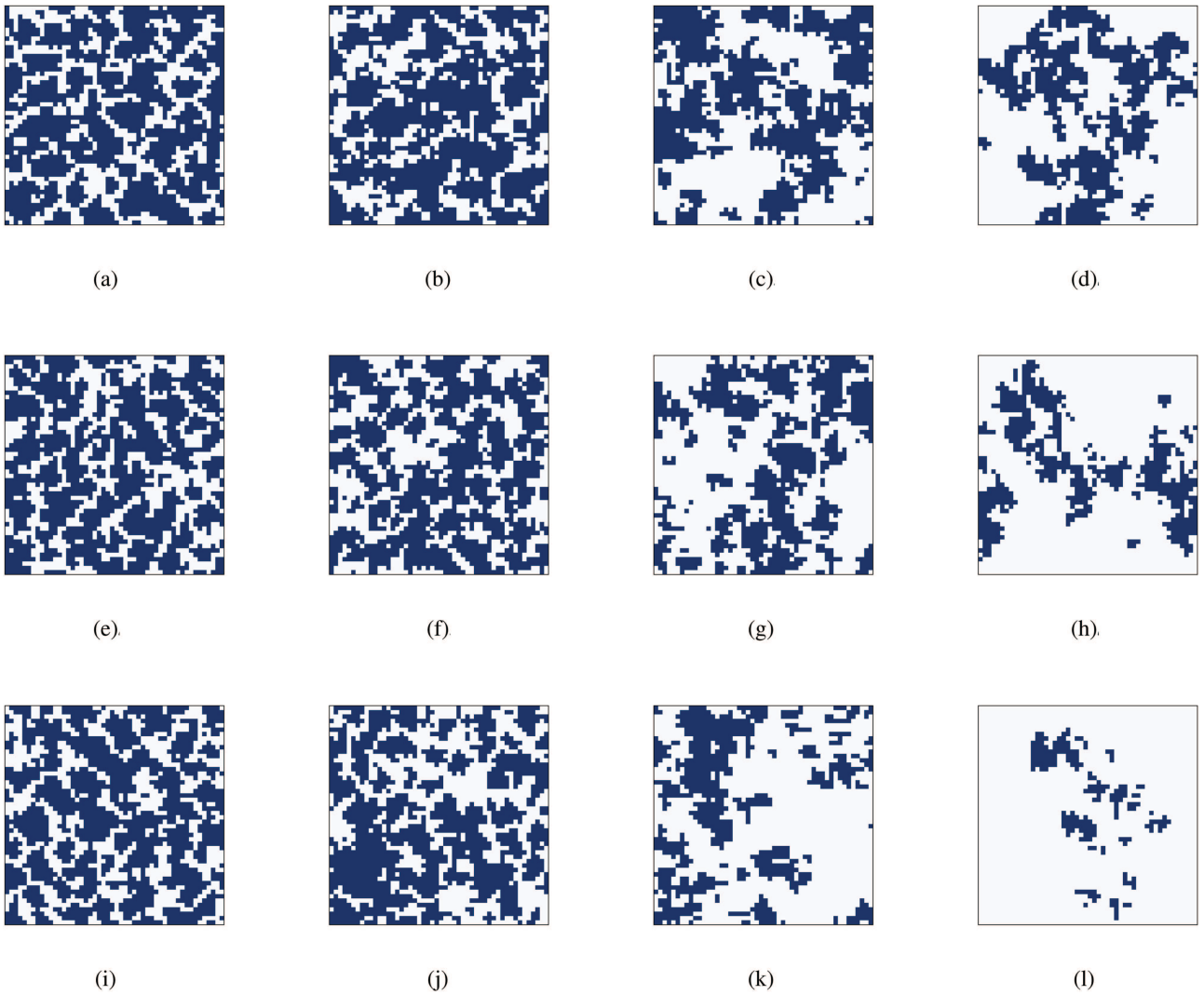

FIG. 3. Cooperation snapshots of WPDs with normal distributed payoffs. The cooperators' clusters usually split up with a high standard deviation in WPDs. This figure presents the snapshots of the evolution of cooperation in the SLs. The game type is the WPD. We set $b = 1.02, 1.03, 1.04$ and $\sigma = 0.10, 0.30, 0.50, 0.70$ for cross simulations. Each snapshot is presented at $t = 5000$ with the SL size $N = 50 \times 50$. The blue and white cells are the cooperators and the defectors, respectively.

cooperation clusters. Although if r is high, the cooperation densities are almost the same as the change of σ, the population is also more likely to form the cooperation clusters with a higher standard deviation σ. Therefore, the individuals promote their neighbors to play the same cooperative strategy and tend to cooperate with their neighbors instead of adopting the opposite strategy in the SDGs with a high standard deviation of their payoffs, which enhances the emergence of cooperation in the population.

3. The population payoffs

By analyzing the individuals' payoffs in the stable state of the networks, we present the boxplots of the individuals' average payoffs in the last 500 time steps in Figs. 5 (WPDs) and 6 (SDGs), respectively. We set $\sigma = 0.10, 0.30, 0.50, 0.70, 0.90$ and investigate the payoff distribution on the four types of networks. It is worth noting that the average payoffs are the average of time instead of each individual's degree. Besides, the numerical difference in the mean payoff comes from the difference in the network structure.

(a) WPDs. In Fig. 5, we show that the medians (red lines) of individuals' payoffs usually decrease as the increase of σs as well as the mean values (green triangles). However, in the HL, there is an increase of both the median and the mean value from $\sigma = 0.10$ to $\sigma = 0.30$, which is shown previously that a slight rise of the cooperation density emerges provided the standard deviation σ is small in HLs. Besides, the upper quartiles and lower quartiles also show this

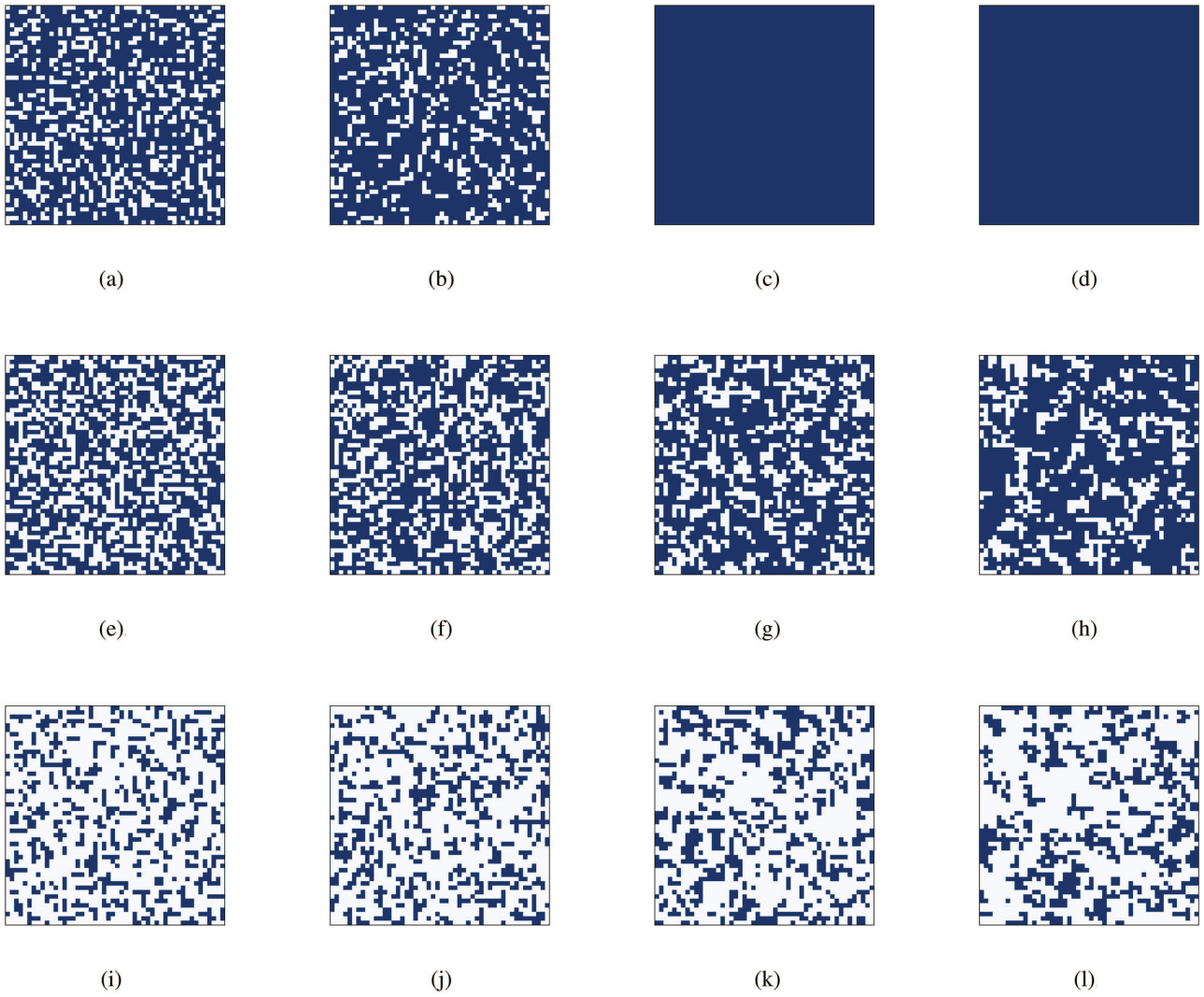

FIG. 4. Cooperation snapshots of SDGs with normal distributed payoffs. The cooperators' clusters usually form with a high standard deviation in SDGs. This figure presents the snapshots of the evolution of cooperation in the SLs. The game type is the SDG. We set $r = 0.25, 0.35, 0.55$ and $\sigma = 0.10, 0.30, 0.50, 0.70$ for cross simulations. Each snapshot is presented at $t = 5000$ with the SL size $N = 50 \times 50$. The blue and white cells are the cooperators and the defectors, respectively.

nature. However, the quartile range does not show any regular pattern in the HL [Fig. 5(a)], the SL [Fig. 5(b)], and the TL [Fig. 5(d)], but becomes smaller as the increase of the standard deviation σ. In addition, for the HL, the SL, and the TL, the number of the large deviation payoff values are small, but for the SW, there are many more large deviation payoffs. And, the large deviation payoff values for the SW are higher than the upper line of the box plot.

(b) SDGs. With the same network types and sizes as above, we then display the boxplots of the population payoff in Fig. 6. As is shown in Figs. 6(a), 6(b), and 6(d), both the upper and the lower quartiles increase as the growth of the standard deviation σ in the HL, the SL, and the TL. Nevertheless, in Fig. 6(c), the individuals' payoffs in the SW are hardly affected by σ's as well as the medians and mean values because of the stability of the cooperation density to the standard deviation σ. Additionally, although the quartile ranges are almost unchanged with the increase of σ, there are many payoff values with large deviation, which is different from the population payoff in the WPDs. In the HL and the SL, there are more individuals who get a smaller payoff than the lower limit of the boxplot. But in the SW, more individuals obtain a higher payoff than the upper limit of the boxplot.

B. Payoffs following the exponential distribution

Then, we focus on the population strategy for WPDs and SDGs with individuals' exponential distributed payoffs.

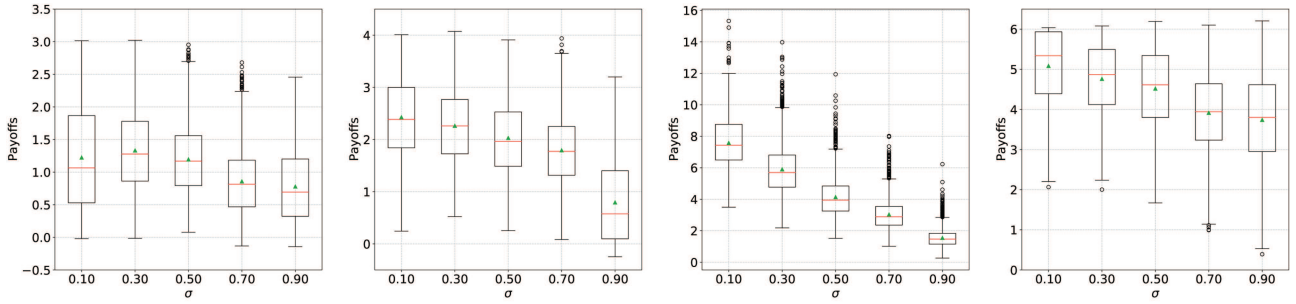

FIG. 5. The boxplots of individuals' average payoffs for WPDs with normal distributed payoffs. The population payoff often decreases with a high standard deviation in WPDs. This figure presents the boxplots of average payoffs in the evolutionary WPDs for $\sigma = 0.10, 0.30, 0.50, 0.70, 0.90$ in the HL [5(a)], the SL [5(b)], the SW [5(c)], and the TL [5(d)]. We set the defector's temptation as $b = 1.03$ in 5(a), 5(b), 5(d) and $b = 1.10$ in 5(c), respectively. The red lines denote the medians, and the green triangles indicate the mean value. The lower and higher lines of the boxes are the lower quartiles and the higher quartiles separately. Each individual's average payoff is obtained by averaging the payoff in the last 500 game rounds in 5000 total rounds.

1. Cooperation density

We now pay attention to the individuals' payoffs that follow the exponential distribution. The results are presented in Fig. 7.

(a) WPDs. We set the range of the horizontal axis as [1.00, 1.30] for a better presentation of the cooperation density in Fig. 7(a). For the WPDs, it is obvious that only the SW and the TL allow the formation of the pure cooperative state, which sustains in the situations with $b < 1.03$ and $b < 1.01$, respectively. However, in the SL and HL, the pure cooperative state does not exist even if the temptation b is small. Besides, there is a rapid phase transition between the pure cooperative state and the pure defective state in the TL, the SL, and the HL, providing less space for the mixed state of cooperators and defectors. Additionally, the SW ensures more chances for the population to have a mixed strategy formation. For the SL and the HL, the cooperation annihilation thresholds are both about 1.07. For the TL, the cooperation annihilation threshold we obtain is approximately 1.11 and is higher than the SL and the HL. For the SW, the value is 1.25, which is much higher than the other three network types. Therefore, the SW provides the best condition in the four types of networks for the emergence of cooperation when the individuals play the WPDs with exponential distributed payoffs.

(b) SDGs. Next, we pay attention to the cooperation density for the SDGs. In Fig. 7(b), we show the plots of cooperation density against the cost-to-benefit ratio r. Generally, the SW provides the best condition for the existence of cooperators, but the worst for the pure cooperative state. On the contrary, the HL provides the largest parameter space for the pure cooperative state, but the narrowest for the mixed strategy state. For the SW, the pure cooperative state sustains until $r = 0.17$, which is the smallest. For the TL and the SL, the defection presence thresholds are 0.25 and 0.30, respectively, and are higher than the SW. And, the highest defection presence threshold is 0.36 in the HL. However, there is a rapid phase transition in the HL from the pure cooperative state to the pure defective state, and the cooperation annihilation threshold is 0.60. The TL and the SL provide the more relaxed condition for the coexistence of

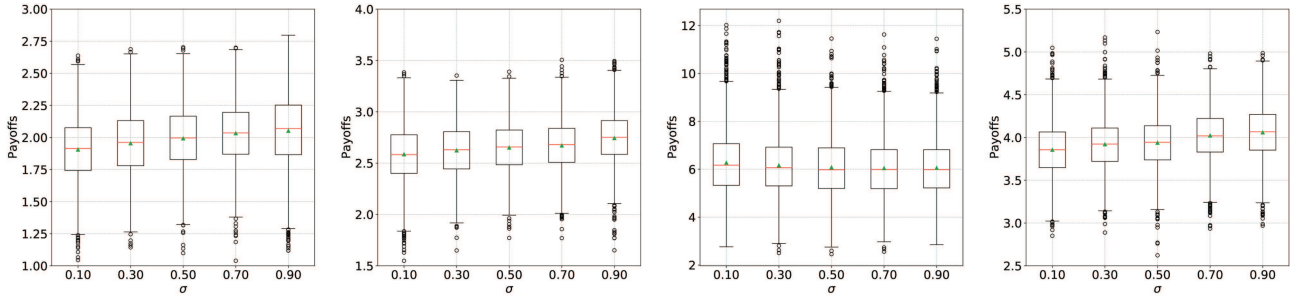

FIG. 6. The boxplots of individuals' average payoffs for SDGs with normal distributed payoffs. The population payoff often increases with a high standard deviation in SDGs. This figure presents the boxplots of average payoffs in the evolutionary SDGs for $\sigma = 0.10, 0.30, 0.50, 0.70, 0.90$ in the HL [5(a)], the SL [5(b)], the SW [5(c)], and the TL [5(d)]. We set the cost-to-benefit ratio as $r = 0.45$ in 5(a)–5(d). The red lines denote the medians, and the green triangles indicate the mean value. The lower and higher lines of the boxes are the lower quartiles and the higher quartiles separately. Each individual's average payoff is obtained by averaging the payoff in the last 500 game rounds in 5000 total rounds.

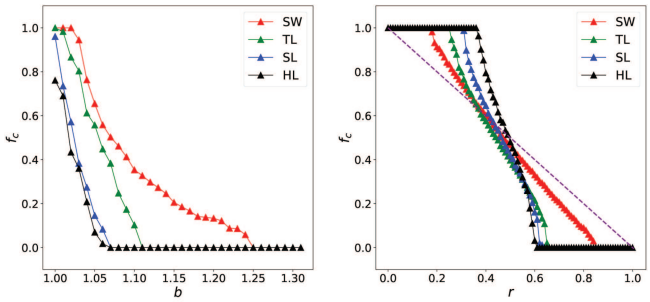

(a) (b)

FIG. 7. Curves of the cooperation density f_c and the game parameters. The SWs provides the largest space for the emergence of cooperators. This figure presents the cooperation density with the change of the game parameters in the SW (red plot), TL (green plot), SL (blue plot), and HL (black plot) when individuals' payoffs follow the exponential distribution. Figures 7(a) and 7(b) show the results for the WPDs and SDGs, respectively. ξ is set as 10^{-6}. The purple plot in Fig. 7(b) presents the equilibrium state in the mixed population without the network structure and variable payoffs. Each cooperation density point is obtained by averaging the last 500 evolution steps in the 5000 total steps.

the cooperators and defectors, where the cooperation annihilation thresholds are 0.65 and 0.63 separately. For the SW, the mixed state of cooperators and defectors sustains a much larger cost-to-benefit ratio, and the cooperation annihilation threshold is 0.84. As shown in previous studies, the equilibrium state for the SDGs in the uniformly mixed population (without any network structure) has $1 - r$ cooperators, presented as the purple plot in Fig. 7(b). Obviously, the cooperation density is increased compared to the uniformly mixed population if the cost-to-benefit ratio r is small (especially for $r < 0.5$). However, the cooperators' percentage reduces with the increase of r. Therefore, we have the conclusion that if the cost-to-benefit ratio is small, the exponential distributed payoff enhances the emergence of cooperation in the SDGs for the four network types we consider. Nevertheless, with the increase of r, the cooperation density becomes smaller than the equilibrium state and quickly drops to the cooperation annihilation state.

2. Cooperation snapshots in SLs

Except the cooperation density, we hope to capture the formation of cooperation clusters. In Fig. 8, we present the snapshots of both the WPDs and the SDGs for several groups of game parameters.

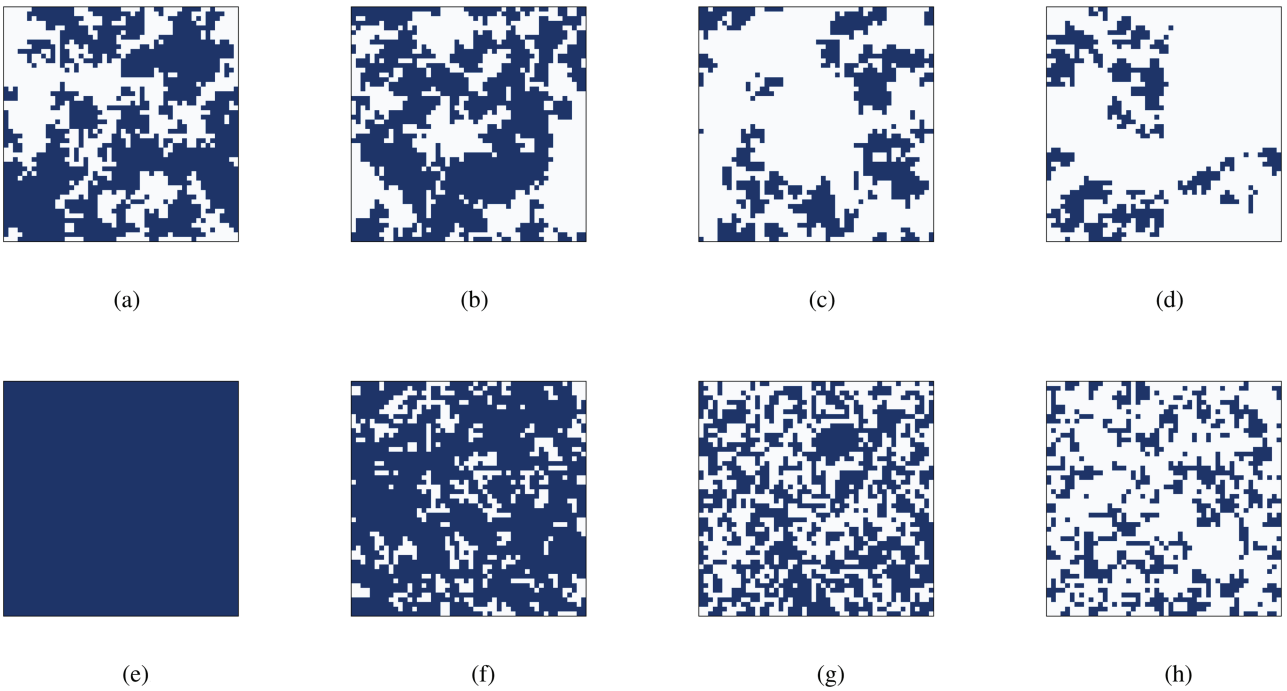

(a) (b) (c) (d)

(e) (f) (g) (h)

FIG. 8. Cooperation snapshots of WPD and SDG with exponential distributed payoffs. The cooperators' cluster split up with the increase of the defector's temptation and the cost-to-benefit ratio. This figure presents the cooperation snapshots in SLs. Figures 8(a)–8(d) show the snapshots for the WPDs with the defector's temptation $b = 1.02, 1.03, 1.04, 1.05$ respectively. Figures 8(e)–8(h) show the snapshots for the SDGs with the cost-to-benefit ratio $r = 0.25, 0.35, 0.45, 0.55$, respectively. Each snapshot is presented at $t = 5000$ with the SL size $N = 50 \times 50$. The blue and white cells are the cooperators and the defectors, respectively.

In Figs. 8(a)–8(d), we display the snapshots of WPDs with the game parameters $b = 1.02, 1.03, 1.04, 1.05$. It is worth noting that the cooperation densities in Fig. 7 are obtained by averaging the last 500 evolution steps in the 5000 total steps. Therefore, the results that we get in Fig. 7 are slightly different from the cooperation densities in the snapshots. The cooperation densities for $b = 1.02$ and 1.03 are 0.5724 and 0.5508 separately. As the defector's temptation b increases to 1.04 and 1.05, the cooperation densities suddenly drop to 0.2748 and 0.1864. Additionally, as the results shown in the population forms the large scale cooperation clusters if the temptation is small, and they split into small cooperation clusters with the increase of b. In Figs. 8(e)–8(h), we show the snapshots of SDGs with the game parameters $r = 0.25, 0.35, 0.45, 0.55$. If the cost-to-benefit ratio $r = 0.25$, there is a pure cooperative state for the whole population. For $r = 0.35$, 0.45, and 0.55, the cooperation densities are 0.7792, 0.5148, and 0.2968, forming fewer cooperation clusters with the increase of r.

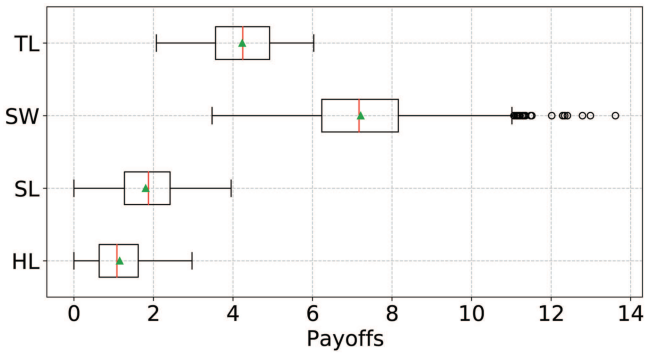

(a)

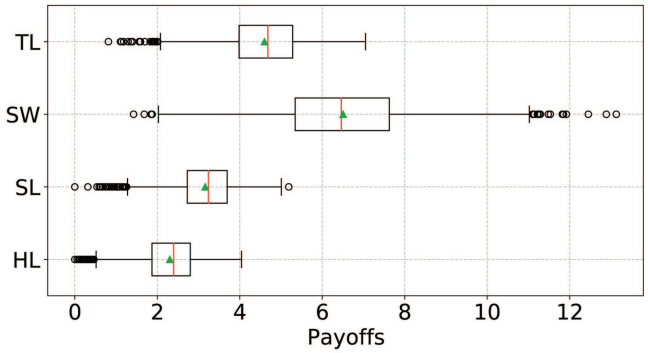

(b)

FIG. 9. The boxplots of individuals' average payoffs for the WPDs and SDGs with normal distributed payoffs. The SWs provide the highest population payoff. This figure presents the boxplots of the population payoff with exponential distributed payoffs for the WPDs [9(a)] and SDGs [9(b)] in the HL, the SL, the SW, and the TL. The defector's temptation for the WPDs is set as $b = 1.03$ [9(a)]. The cost-to-benefit ratio for the SDGs is set as $r = 0.40$ [9(b)]. The red lines denote the medians, and the green triangles are the mean values. Each individual's payoff data are averaged by the last 500 time steps in the 5000 total steps.

3. The population payoffs

Next, we focus on the population payoff for the WPDs and SDGs in the four types of networks we employ in Fig. 9. In Fig. 9(a), we present the results for the WPDs, where the SW provides the individuals with the highest payoff median and mean value. Additionally, the TL supplies the chances for the population to obtain a higher overall payoff than the SL, and the SL offers a better condition for the population payoff than the HL. It is worth emphasizing again that the difference in individuals' payoff comes from the different network structures. Besides, some individuals' payoffs are of large deviation from the medians, which is similar to our results for the WPDs with individuals' normal distributed payoffs in Fig. 5(c). For the results of SDGs in Fig. 9(b), the order of the payoff medians and the mean values is the same as that of WPDs in Fig. 9(a), and we have SW > TL > SL > HL. It is worth noting that when playing SDGs, the large deviation payoff emerges more and is similar to our results for the normal distributed payoff in Fig. 6. Additionally, the payoff with a large deviation is usually smaller than the lower limit of each box in the TL, the SL, and the HL. However, in the SW, there are more values higher than the upper limit. And, for both WPDs and SDGs, the population payoffs have the largest quartile range. That is to say, the SW provides both the widest cooperation space and the highest payoff for the population when playing the WPDs and SDGs.

IV. CONCLUSION AND OUTLOOK

In this paper, we study the evolution of cooperation with stochastic risks, considering the individuals' payoffs as variables that follow a specific probability distribution with a fixed expectation. Two types of probability distribution function are considered in our study, including the normal distribution, for which the expected payoff does not influence the risk, and the exponential distribution, where the expected payoff does influences the risk and especially if the expected payoff is higher than the mutual cooperation. In simulations, we perform the evolution process on WPDs and SDGs and focus on the cooperation density and the formation of the cooperation clusters. We find that if the individuals' payoffs follow the normal distribution, the greater standard deviation σ usually inhibits the emergence of cooperators for the WPDs, but promotes the cooperation for the SDGs. By studying the cooperation snapshots in SLs, we suggest that the cooperation clusters split when individuals play the WPDs with a large σ, which decreases the cooperation density. Besides, if the individuals play the SDGs, the filamentous cooperators agglomerate with a large σ and enhances the emergence of the cooperation clusters. For the individuals interact with their neighbors with the exponential distributed payoffs, we conclude that the SW provides the best condition for both the pure cooperative state and the mixed strategy state while the HL provides the worst as the individuals play the WPDs. For the SDGs, we find that the SW provides the best condition for the coexistence of the cooperators and the defectors but the worst for the pure cooperation state. Additionally, the HL guarantees the largest space for the pure cooperation state but the fastest phase transition from the pure cooperation to the pure defection state.

Based on our work, there are some extensions to investigate more information for the spatial evolution of cooperation with

stochastic risks. For example, there are other probability distribution function to measure the stochastic risk in the population, such as the log-normal distribution and the power-law distribution. Besides, we study the cooperation density in 4 network types by the pairwise interaction strategy update among the population. There can be some dominant conditions of cooperation in the population by the birth–death process, the death–birth process, and the pairwise interaction, which is related to the network structure and the game model. All these issues will be studied in our future work.

ACKNOWLEDGMENTS

This document is the results of the research project funded by the Humanities and Social Science Fund of Ministry of Education of the People's Republic of China under Grant No. 21YJCZH028.

AUTHOR DECLARATIONS

Conflict of Interest

The authors have no conflicts to disclose.

Author Contributions

Ziyan Zeng: Conceptualization (lead); Data curation (lead); Formal analysis (lead); Investigation (equal); Methodology (lead); Resources (equal); Software (lead); Validation (equal); Writing – original draft (lead); Writing – review and editing (equal). **Qin Li:** Conceptualization (equal); Data curation (equal); Funding acquisition (equal); Investigation (lead); Methodology (equal); Supervision (equal); Validation (equal); Writing – original draft (equal); Writing – review and editing (equal). **Minyu Feng:** Funding acquisition (lead); Methodology (equal); Project administration (lead); Resources (lead); Supervision (lead); Validation (equal); Writing – review and editing (lead).

DATA AVAILABILITY

The data that support the findings of this study are available from the corresponding author upon reasonable request.

REFERENCES

[1]X.-D. Zheng, C. Li, S. Lessard, and Y. Tao, "Environmental noise could promote stochastic local stability of behavioral diversity evolution," Phys. Rev. Lett. **120**(21), 218101 (2018).
[2]T.-J. Feng, J. Mei, C. Li, X.-D. Zheng, S. Lessard, and Y. Tao, "Stochastic evolutionary stability in matrix games with random payoffs," Phys. Rev. E **105**(3), 034303 (2022).
[3]P. Richerson, R. Boyd, and J. Henrich, "Human cooperation," Genet. Cult. Evol. Coop. **17**, 413–425 (2003).
[4]R. Boyd and P. J. Richerson, "Culture and the evolution of human cooperation," Philos. Trans. R. Soc. B: Biol. Sci. **364**(1533), 3281–3288 (2009).
[5]J. Tanimoto, *Fundamentals of Evolutionary Game Theory and Its Applications* (Springer, 2015).
[6]K. Sigmund and M. A. Nowak, "Evolutionary game theory," Curr. Biol. **9**(14), R503–R505 (1999).
[7]L. Sagiv, N. Sverdlik, and N. Schwarz, "To compete or to cooperate? Values' impact on perception and action in social dilemma games," Eur. J. Social Psychol. **41**(1), 64–77 (2011).
[8]A. Rappoport and A. M. Chammah, *Prisoner's Dilemma* (University of Michigan Press, Ann Arbor, 1965).
[9]C. A. Holt and A. E. Roth, "The nash equilibrium: A perspective," Proc. Natl. Acad. Sci.U.S.A. **101**(12), 3999–4002 (2004).
[10]M. A. Nowak and R. M. May, "Evolutionary games and spatial chaos," Nature **359**(6398), 826–829 (1992).
[11]G. Szabó and G. Fath, "Evolutionary games on graphs," Phys. Rep. **446**(4–6), 97–216 (2007).
[12]C. Hauert and M. Doebeli, "Spatial structure often inhibits the evolution of cooperation in the snowdrift game," Nature **428**(6983), 643–646 (2004).
[13]F. C. Santos and J. M. Pacheco, "Scale-free networks provide a unifying framework for the emergence of cooperation," Phys. Rev. Lett. **95**(9), 098104 (2005).
[14]M. A. Nowak, "Five rules for the evolution of cooperation," Science **314**(5805), 1560–1563 (2006).
[15]M. Perc and A. Szolnoki, "Coevolutionary games—A mini review," BioSystems **99**(2), 109–125 (2010).
[16]S. Boccaletti, G. Bianconi, R. Criado, C. I. Del Genio, J. Gómez-Gardenes, M. Romance, I. Sendina-Nadal, Z. Wang, and M. Zanin, "The structure and dynamics of multilayer networks," Phys. Rep. **544**(1), 1–122 (2014).
[17]S. Boccaletti, V. Latora, Y. Moreno, M. Chavez, and D.-U. Hwang, "Complex networks: Structure and dynamics," Phys. Rep. **424**(4–5), 175–308 (2006).
[18]M. Kivelä, A. Arenas, M. Barthelemy, J. P. Gleeson, Y. Moreno, and M. A. Porter, "Multilayer networks," J. Comp. Netw. **2**(3), 203–271 (2014).
[19]P. Holme and J. Saramäki, "Temporal networks," Phys. Rep. **519**(3), 97–125 (2012).
[20]A. Li, S. P. Cornelius, Y.-Y. Liu, L. Wang, and A.-L. Barabási, "The fundamental advantages of temporal networks," Science **358**(6366), 1042–1046 (2017).
[21]A. R. Benson, D. F. Gleich, and J. Leskovec, "Higher-order organization of complex networks," Science **353**(6295), 163–166 (2016).
[22]R. Lambiotte, M. Rosvall, and I. Scholtes, "From networks to optimal higher-order models of complex systems," Nat. Phys. **15**(4), 313–320 (2019).
[23]M. Jusup, P. Holme, K. Kanazawa, M. Takayasu, I. Romić, Z. Wang, S. Geček, T. Lipić, B. Podobnik, L. Wang, W. Luo, T. Klanjček, J. Fan, S. Boccaletti, and M. Perc, "Social physics," Phys. Rep. **948**, 1–148 (2022).
[24]Z. Wang, L. Wang, A. Szolnoki, and M. Perc, "Evolutionary games on multilayer networks: A colloquium," Eur. Phys. J. B **88**(5), 1–15 (2015).
[25]D. Y. Kenett, M. Perc, and S. Boccaletti, "Networks of networks—An introduction," Chaos Solitons Fractals **80**, 1–6 (2015).
[26]A. Li, L. Zhou, Q. Su, S. P. Cornelius, Y.-Y. Liu, L. Wang, and S. A. Levin, "Evolution of cooperation on temporal networks," Nat. Commun. **11**(1), 1–9 (2020).
[27]N. Perra, B. Gonçalves, R. Pastor-Satorras, and A. Vespignani, "Activity driven modeling of time varying networks," Sci. Rep. **2**(1), 1–7 (2012).
[28]H. Guo, D. Jia, I. Sendiña-Nadal, M. Zhang, Z. Wang, X. Li, K. Alfaro-Bittner, Y. Moreno, and S. Boccaletti, "Evolutionary games on simplicial complexes," Chaos Solitons Fractals **150**, 111103 (2021).
[29]U. A. Rodriguez, F. Battiston, G. F. de Arruda, Y. Moreno, M. Perc, and V. Latora, "Evolutionary dynamics of higher-order interactions in social networks," Nat. Hum. Behav. **5**(5), 586–595 (2021).
[30]Y. Zhang, H. Ning, J. Wang, and C. Xia, "Coveting the successful neighbor promotes the cooperation for the spatial public goods game on two-layered lattices," Chaos Solitons Fractals **105**, 29–37 (2017).
[31]D. Han, S. Yan, and D. Li, "The evolutionary public goods game model with punishment mechanism in an activity-driven network," Chaos Solitons Fractals **123**, 254–259 (2019).
[32]A. Civilini, N. Anbarci, and V. Latora, "Evolutionary game model of group choice dilemmas on hypergraphs," Phys. Rev. Lett. **127**(26), 268301 (2021).
[33]Q. Su, A. McAvoy, L. Wang, and M. A. Nowak, "Evolutionary dynamics with game transitions," Proc. Natl. Acad. Sci. U.S.A. **116**(51), 25398–25404 (2019).
[34]M. Perc, "Coherence resonance in a spatial prisoner's dilemma game," New J. Phys. **8**(2), 22 (2006).
[35]M. Perc, "Transition from gaussian to levy distributions of stochastic payoff variations in the spatial prisoner's dilemma game," Phys. Rev. E **75**(2), 022101 (2007).
[36]Z. Zeng, Y. Li, and M. Feng, "The spatial inheritance enhances cooperation in weak prisoner's dilemmas with agents—Exponential lifespan," Physica A **593**, 126968 (2022).

[37]B. Pi, Z. Zeng, M. Feng, and J. Kurths, "Evolutionary multigame with conformists and profiteers based on dynamic complex networks," Chaos **32**(2), 023117 (2022).
[38]M. Feng, Y. Li, F. Chen, and J. Kurths, "Heritable deleting strategies for birth and death evolving networks from a queueing system perspective," IEEE Trans. Syst. Man Cybern. Syst. (published online, 2022).
[39]Y. Li, Z. Zeng, M. Feng, and J. Kurths, "Protection degree and migration in the stochastic SIRS model: A queueing system perspective," IEEE Trans. Circuits Syst. I: Regul. Pap. **69**(2), 771–783 (2021).
[40]M. Feng, L. Deng, and J. Kurths, "Evolving networks based on birth and death process regarding the scale stationarity," Chaos **28**(8), 083118 (2018).
[41]M. Perc and A. Szolnoki, "Social diversity and promotion of cooperation in the spatial prisoner's dilemma game," Phys. Rev. E **77**(1), 011904 (2008).
[42]M. A. Amaral, L. Wardil, M. Perc, and J. K. L. da Silva, "Evolutionary mixed games in structured populations: Cooperation and the benefits of heterogeneity," Phys. Rev. E **93**(4), 042304 (2016).
[43]J. K. Patel and C. B. Read, *Handbook of the Normal Distribution* (CRC Press, 1996), Vol. 150.